Thermochemistry of $N_3O_2^-$

John W. Torchia,[†] Kelly O. Sullivan,[‡] and Lee S. Sunderlin*[,†]

Department of Chemistry and Biochemistry, Northern Illinois University, DeKalb Illinois 60115, and Department of Chemistry, Creighton University, Omaha Nebraska 68178

Received: July 8, 1999; In Final Form: October 1, 1999

$N_3O_2^-$ has been formed by the addition of 0.4 Torr of N_2O to a flowing afterglow apparatus. Energy-resolved collision-induced dissociation of this anion gives NO^- as the dominant product. O^- and N_2O^- are also observed, and there is indirect evidence for electron detachment. The $NO^- - N_2O$ bond energy at 0 K is measured to be 0.76 ± 0.10 eV. Ab initio calculations at the MP2/aug-cc-pVDZ level give a bond strength of 0.78 eV, in good agreement with the experimental results. The predominance of NO^- over N_2O^- is consistent with a metastable N_2O^- anion. The results suggest that dissociative photodetachment of $N_3O_2^-$ gives highly internally excited products.

Introduction

The oxides of nitrogen are known for their unusual electronic properties. For example, NO has a remarkably small electron affinity of 0.026 eV[1] (1 eV = 96.485 kJ/mol). NO^- is classically unbound, and zero point energy effects are responsible for the positive electron affinity.[2] N_2O, on the other hand, has a electron affinity of −0.15 eV;[3] N_2O^- is metastable because of the large geometry difference between the bent anion (bond angle 133°)[3] and the linear structure of neutral N_2O. This study explores the thermodynamics of the anionic heterodimer of these two species, $N_3O_2^-$.

The dinitrosoamide anion,[4] $N_3O_2^-$, is a terminal ion observed in the reactions of nitrogen oxides. Moruzzi and Dakin[5] first observed $N_3O_2^-$ in drift cell experiments, and postulated the following mechanism.

$$NO^- + N_2O \rightleftarrows (N_3O_2^-)^* \quad (1)$$

$$(N_3O_2^-)^* + N_2O \rightarrow N_3O_2^- + N_2O \quad (2)$$

Parkes[6] observed $N_3O_2^-$ as a product of an overall third-order reaction of NO^- with N_2O and either CO_2 or another N_2O molecule (reactions 3 and 4) and measured the rate constant

$$NO^- + N_2O + CO_2 \rightarrow N_3O_2^- + CO_2 \quad (3)$$

$$NO^- + 2N_2O \rightarrow N_3O_2^- + N_2O \quad (4)$$

$$NO^- + N_2O + Ar \rightarrow N_3O_2^- + Ar \quad (5)$$

for reaction 4 as $k_4 = 8.5 \times 10^{-30}$ cm^6 s^{-1} at 298 K. Viggiano and co-workers[7] measured a moderately negative temperature dependence for reaction 4, consistent with the presumed temperature dependence of the equilibrium for reaction 1. At 193 K, Ferguson and co-workers measured a very similar rate constant of 7.1×10^{-30} cm^6 s^{-1} for reaction 5, the analogous association reaction with Ar as the third body.[8] The effectiveness of argon in promoting formation of $N_3O_2^-$ suggests that the third body acts as a collisional cooling agent rather than a catalyst.

Recent work has suggested that there are several isomers for the $N_3O_2^-$ anion.[9] Coe et al. observed a weakly bound $(NO^-)N_2O$ cluster, identified by a photoelectron spectra very similar to that seen for NO^-.[10] A bond energy of 0.22 eV was estimated from the shift in the peaks of the spectra. Hayakawa et al. observed $N_3O_2^-$ but not NO^- in an N_2O buffer at atmospheric pressure at temperatures from 300 to 500 K,[11] indicating that ΔG for reaction 4 is negative in this temperature range. This demonstrates the existence of an $N_3O_2^-$ isomer with a bond enthalpy significantly stronger than 0.22 eV.

Continetti and co-workers[12] studied $N_3O_2^-$ using coincident photoelectron and photofragment translational spectroscopy. They observed the weakly bound complex seen by Coe et al., as well as at least one more strongly bound isomer. For a photon energy of 4.66 eV, the maximum total (electron + neutral fragment) translational energy release observed was 2.7 eV. Continetti et al. reported the difference between these two energies, 2.0 ± 0.2 eV, as the stability of $N_3O_2^-$ relative to the decomposition products of NO, N_2O, and e^-. They derived this value on the assumption "... that some of the NO + N_2O products are produced with no internal excitation...."[12] For a photon energy of 3.49 eV, the maximum neutral fragment translational energy was ca. 1.5 eV, again around 2.0 eV less than the photon energy. However, for a photon energy of 2.33 eV, the maximum neutral fragment translational energy release was ca. 1 eV. This suggests that an isomer with a maximum bond energy of ca. 1.3 eV exists. The small signal for this feature in the translational energy spectra is consistent with a minor isomer.

Computational studies of this molecule have been limited. Hiraoka et al. obtained bond energies of 1.25 eV for singlet, covalently bound $N_3O_2^-$ and 0.21 eV for a triplet $NO^- - N_2O$ cluster at the MP2/6-31+G(d)//R(O)HF/6-31+G level.[9] Density functional calculations by Pápai and Stirling[13] indicate that neutral N_3O_2 is covalently bound, but unstable with respect to NO + N_2O by 1.17 eV.

* Corresponding author. Phone: 815-753-6870. Fax: 815-753-4802. E-mail: sunder@niu.edu.
[†] Northern Illinois University.
[‡] Creighton University.

10.1021/jp992289g CCC: $18.00
Published on Web 11/11/1999

This study was undertaken to measure the bond energy in $N_3O_2^-$ through a different route, namely determining the translational energy required for collision-induced dissociation. Further ab initio calculations have also been performed, both to aid in the experimental data analysis and to confirm the thermochemical conclusions.

Experimental Section

The flowing afterglow tandem mass spectrometer used in these experiments consists of an ion source, a flow reactor, and a tandem mass spectrometer comprising a quadrupole mass filter, an octopole ion guide,[14] a second quadrupole mass filter, and a detector. This instrument has been described in detail previously;[15] a brief description follows.

The flow tube is a 92 cm × 7.3 cm i.d. stainless steel pipe with five neutral reagent inlets. Usually, the bulk of the gas in the flow tube is He, and ion precursors are present in trace amounts. In the present experiments, partial pressures of 0.3−0.5 Torr of N_20 and 0.0−0.2 Torr of helium were used. The ion signal was strongly dependent on the pressure of N_2O, and nearly independent of the pressure of He. This behavior is consistent with the kinetics observed previously.[6]

The ion source is a dc discharge typically operated at 1500 V with 4 mA of emission current. The gas flow velocity is 40 m/s when the buffer gas is mostly N_2O, giving over 10^5 collisions with the neutral N_2O or He to thermalize the ions.

Ions are sampled from the flow tube into the main chamber, which contains the tandem mass spectrometer. This chamber is differentially pumped to pressures sufficiently low that further collisions of the ions with the buffer gas are unlikely. The operating conditions for the first quadrupole were set to ensure that only ions of $m = 74$ u were allowed to pass into the octopole, which passes through a gas cell filled with argon for the CID experiments. The intensities of the products and unreacted ions are measured by the second quadrupole and the electron multiplier detector. The resolution of the second quadrupole was left as low as possible to improve collection efficiency and reduce mass discrimination. These operating conditions gave typically 50 000 ions s^{-1} of the $N_3O_2^-$ reactant.

Threshold Analysis. The threshold energy for a reaction is determined by modeling the intensity of product ions as a function of the reactant ion kinetic energy in the center-of-mass (CM) frame, E_{CM}. The translational energy zero of the reactant ion beam is measured using the octopole as a retarding field analyzer.[14,16] The first derivative of the beam intensity as a function of energy is approximately Gaussian, with a full-width at half-maximum of typically 1.0 eV for these experiments. The laboratory energy E_{lab} is given by the octopole rod offset voltage measured with respect to the center of the Gaussian fit. Conversion to the CM frame is accomplished by use of $E_{CM} = E_{lab}m/(m + M)$, where m and M are the masses of the neutral and ionic reactants, respectively. This energy is corrected at low offset energies to account for truncation of the ion beam.[16]

Total cross sections for reaction, σ_{total}, are calculated using $I = I_0 \exp(-\sigma_{total}nl)$,[16] where I is the intensity of the reactant ion beam, I_0 is the intensity of the incoming ion beam ($I_0 = I + \Sigma I_i$), and I_i are the intensities for each product ion. The number density of the neutral collision gas is n, and l is the effective collision cell length, 13 ± 2 cm.[15] Individual product cross sections σ_i are equal to $\sigma_{total}(I_i/\Sigma I_i)$.

To derive CID threshold energies, the threshold region of the data is fit with the model function given in eq 6,[17] where $\sigma(E)$ is the cross section for formation of the product ions

$$\sigma(E) = \sigma_o \Sigma_i [g_i P_D(E,E_i)(E + E_i - E_T)^n/E] \quad (6)$$

at center-of-mass energy E, E_T is the desired threshold energy, σ_o is a scaling factor, n is an adjustable parameter, P_D is the probability of an ion with a given amount of energy dissociating within the experimental window (ca. 30 μs), and i denotes rovibrational states having energy E_i and population g_i ($\Sigma g_i = 1$). The CRUNCH program written by Professor P. B. Armentrout and co-workers is used in the threshold analysis described above.[16] Doppler broadening, the kinetic energy distribution of the reactant ion, and the competition between multiple dissociation pathways are also accounted for by the CRUNCH program.

P_D is calculated using the RRKM formalism. If it is assumed that the transition state for loss of N_2O is loose (product-like), the calculated effect of delayed dissociation (the kinetic shift) is less than 0.01 eV. It is possible that a change of spin from reactants to products (discussed below) leads to inefficient dissociation. However, even assuming that the dissociation efficiency is a factor of 10^6 less than predicted by RRKM, the kinetic shift is still less than 0.01 eV. Thus, the kinetic shift is negligible for this system.

The collision gas pressure can influence the observed cross sections because of secondary collisions. This is accounted for by linear extrapolation of data taken at several pressures to a zero pressure cross section.[18] The uncertainty in the reaction thresholds due to the internal energy of the reactant ions is estimated by determining the threshold by assuming all of the calculated frequencies are in error by ±10%. Also, the uncertainty in the energy scale is 0.15 eV in the lab frame. These uncertainties are combined with the standard deviation of the thresholds derived from different data sets to give the overall uncertainty in reaction energetics.

Collisional reheating can potentially affect the measured thresholds. This occurs when ions gain energy from collisions with the buffer gas during extraction from the flow tube. While this is generally not a problem for light buffer gases such as He, the use of a high pressure of N_2O means that collisional heating is more likely. Changing the accelerating potentials on the first few ion optics elements, where the ions are extracted from the flow tube, had no measurable effect on the observed reaction threshold, suggesting that collisional reheating is minor for the present experiments.

Computational Methods. All ab initio calculations were performed using the GAUSSIAN94 suite of programs[19] running on a Digital Alpha 433au workstation. Calculations were performed using Dunning's aug-cc-pVDZ basis set for nitrogen and oxygen.[20] This double-ζ quality set is formed from a (9s4p1d) primitive set contracted to [3s2p1d] and augmented by a diffuse (1s1p1d) set. Spherical harmonic forms for the d functions were employed. Electron correlation was built onto UHF wave functions using the MP2 level of theory. Analytic gradients were used to optimize the geometry and determine the vibrational frequencies of all isomers calculated. The stability was determined by comparison to an asymptotic limit of $NO^- + N_2O$ calculated at the same level. Both singlet and triplet isomers were investigated.

Results

Electron impact on N_2O in He gives predominantly $N_3O_2^-$ at sufficiently high flow rates of N_2O, consistent with the previous results discussed above. The cross sections for CID of $N_3O_2^-$ with Ar are shown in Figure 1. The three products observed correspond to reactions 7−9, where the neutral

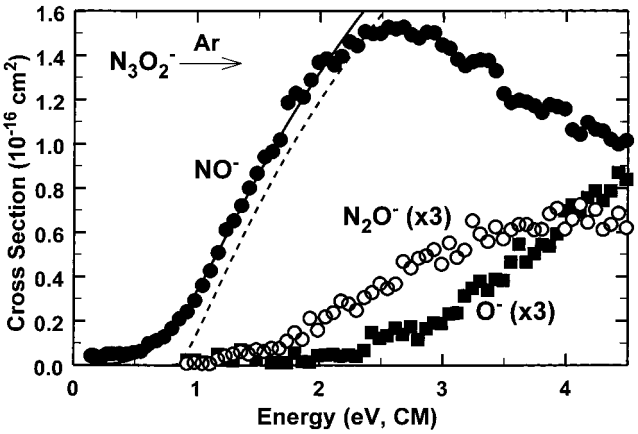

Figure 1. Appearance curves for collision-induced dissociation of $N_3O_2^-$ as a function of kinetic energy in the center-of-mass frame. The solid lines are convoluted fits to the data, and the dashed lines are unconvoluted fits to the data. The fitting parameters for this data set are $E_T = 0.84$ eV and $n = 1.4$. See text for a discussion of the fitting parameters.

TABLE 1: Molecular Constants[a]

molecule	vibrational frequency	rotational constant
$N_3O_2^-$ (w-shaped)	196, 327, 343, 604, 755, 1146, 1256, 1433, 1502	1.96, 0.0929, 0.0887
NO[b]	1924	1.68 (×2)
NO^- [b]	1290	1.39 (×2)
N_2O[c]	590 (×2), 1274, 2258	0.403 (×2)
N_2O^- [c]	623, 916, 1662	6.87, 0.410, 0.386

[a] Constants in cm^{-1} calculated at the MP2/aug-cc-pVDZ level unless otherwise noted. [b] QCISD(T)/aug-cc-pVTZ results from ref 2. [c] QCISD(T)/aug-cc-pVTZ results from ref 3.

products are assumed on thermodynamic grounds. The apparent threshold for reaction is somewhat below 1 eV. The products seen correspond to the ions observed after the ~30 μs time between collisional activation and product detection.

$$N_3O_2^- \rightarrow NO^- + N_2O \quad (7)$$

$$\rightarrow NO + N_2O^- \quad (8)$$

$$\rightarrow NO + N_2 + O^- \quad (9)$$

Computational results for $N_3O_2^-$ are given in Tables 1 and 2 and in Figure 2. The stationary points found include two singlet and two triplet structures. The lowest singlet structure has a "W" geometry with C_{2v} symmetry, while the higher energy isomer is nonplanar. The calculated D_e of 0.876 eV is smaller than the 1.25 eV bond strength previously calculated at a lower level of theory.[9] The two triplet structures are nearly equal in energy and correspond to rotamers of a weakly bound $NO^-\cdot N_2O$ complex. N_2O has singlet spin, but the ground state of NO^- has a triplet spin like the isoelectronic O_2 molecule. Thus, a singlet−triplet crossing is necessary for formation of $N_3O_2^-$ from ground-state $NO^- + N_2O$, as well as for CID of $N_3O_2^-$ to form ground-state products.

Discussion

Cross Section Modeling. The best fit to the experimental data for reaction 7 is also shown in Figure 1. The fitting parameters used are $n = 1.4 \pm 0.2$ and $E_T = 0.76 \pm 0.08$ eV. Including uncertainties of 0.005 eV for the effect of varying the vibrational frequencies and 0.053 eV for the energy scale uncertainty in the CM frame, the threshold value is 0.76 ± 0.10 eV (73 ± 10 kJ/mol). Because the reactant and product internal energies are explicitly accounted for in the model, the derived threshold corresponds to a 0 K bond energy. Calculating the necessary heat capacities using the ab initio vibrational frequencies, the bond enthalpy at 298 K is 79 ± 10 kJ/mol.

TABLE 2: Calculated Bond Energies[a]

molecule	D_e	D_o, 0 K
singlet planar $N_3O_2^-$	0.876	0.780
singlet nonplanar $N_3O_2^-$	0.497	0.412
triplet planar $NO^-\cdot N_2O$	0.139	0.113
triplet nonplanar $NO^-\cdot N_2O$	0.143	0.118
$NO^- + N_2O$	0	0

[a] Values in eV calculated at the MP2/aug-cc-pVDZ level.

The experimental bond energy is in good agreement with the computed 0 K bond energy of 0.78 eV (75 kJ/mol) for the singlet W-shaped isomer. The nonplanar singlet structure is calculated to be 0.37 eV higher in energy. Assuming the two singlet isomers are in equilibrium at the flow tube temperature, the abundance of the lower-energy isomer is roughly 10^6 greater than that of the higher isomer. Thus, the metastable singlet isomer is probably not significant in these experiments. Coe et al.[10] observed a weakly bound isomer, which was estimated to be bound by 0.22 eV. The computational results indicate that the two triplet rotamers are bound by 0.11−0.12 eV at 0 K. Thus, the structure observed by Coe et al. is presumably some mixture of these triplets. (The energy resolution of the PES data is such that the two species would be indistinguishable.)

Ion Source Conditions and Ion Populations. At this point, the ion source conditions in the different experiments can be correlated with the ions produced. It is reasonable to assume that the intermediate included in reactions 1 and 2 is the loosely bound triplet complex. In the supersonic expansions used by Coe et al.[10] and Resat et al.[12] both the triplet complex and the singlet covalent isomer are apparently produced. The weakly bound cluster is evident in the PES data from both groups, while the covalent isomer is only apparent in the electron energy/neutral translational energy coincidence measurements. The relatively low temperature in the expansion as well as the initially high pressure of N_2O are consistent with a significant concentration of the triplet complex. For the room temperature, lower pressure experimental conditions used in this study, entropy effects ensure that the equilibrium for reaction 1 lies far to the left, and the population of the loosely bound cluster in the ions exiting the flow tube is negligible. Instead, most of the ions seen under flow tube conditions should be the covalent singlet, which accumulates intensity over the length of the flow tube. Formation of the strongly bound covalent isomer in the present experiments is consistent with the previous flow tube and high-pressure mass spectrometry results.

If a significant population of the higher-energy isomers existed in the ion beam, then there should be secondary features in the CID data at low energy. The absence of such features indicates that the loosely bound complex is a negligible fraction of the ion population. Similar results have apparently been observed for $N_2H_2O_2^+$ systems, where a thermal (flow tube) ion source produced strongly bound $[N_2O\cdot H_2O]^+$ ions while a cooler supersonic jet source also produced more loosely bound cluster ions.[21]

Electron Detachment. The thermodynamic threshold for reaction 8 is only slightly higher than the threshold for reaction 7. Reaction 8 is also entropically favored over reaction 7 because the products have one more rotational degree of freedom. Furthermore, spin is conserved in reaction 8, while reaction 7

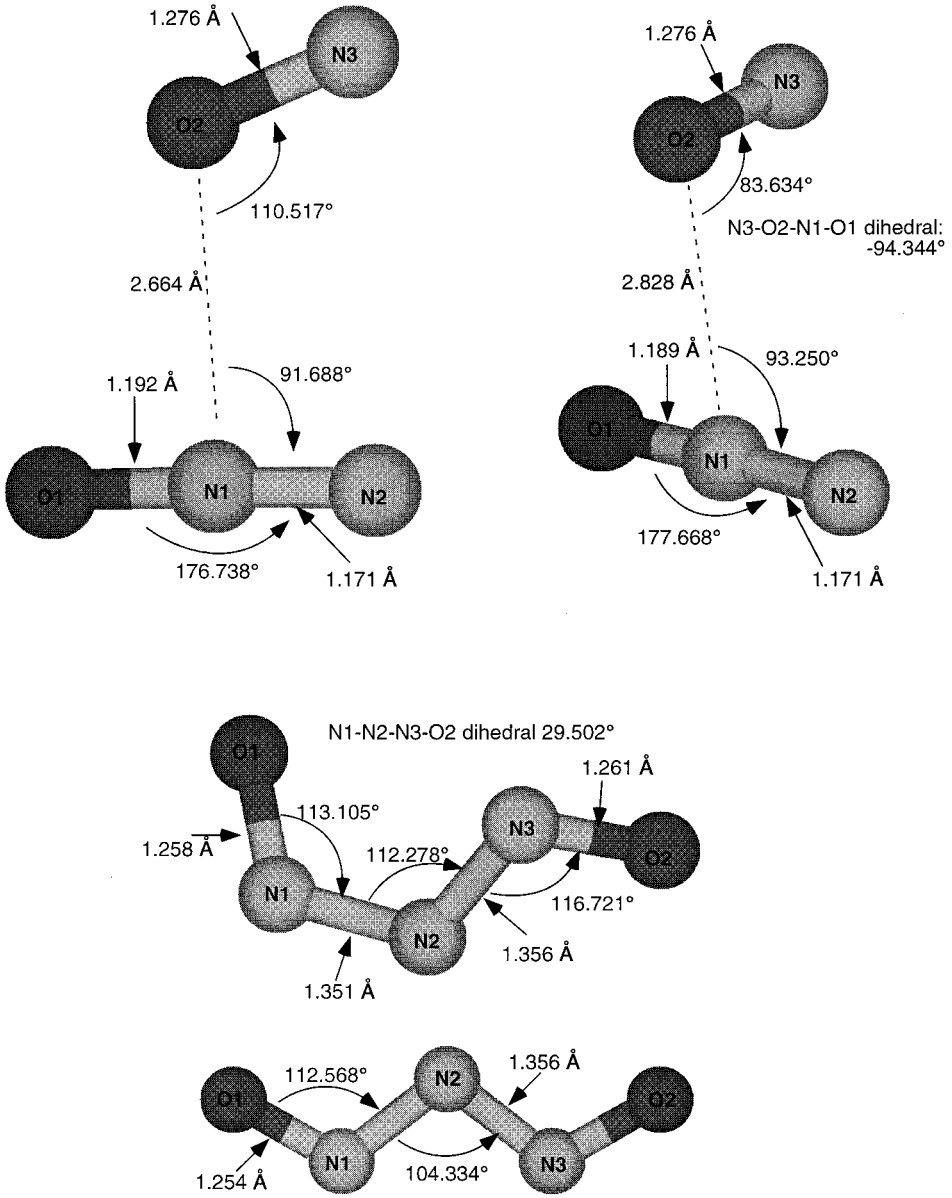

Figure 2. Stationary point geometries for isomers of $N_3O_2^-$ calculated at the MP2/aug-cc-pVDZ level. The cluster structures are triplets, while the covalent structures are singlets.

involves a ground-state singlet reactant and ground-state triplet products. Thus, formation of N_2O^- should be reasonably competitive with formation of NO^- over the energy range studied. Instead, the cross section for reaction 8 is always at least a factor of 4 smaller than that for reaction 7. There are two plausible causes for this. If N_2O^- is formed with a significant amount of vibrational excitation, it is likely to lose an electron, as discussed previously. Also, N_2O^- can lose O^-, observed as reaction 9. Attempts to model reaction 8 or reactions 8 and 9 together using statistical models for the reaction probabilities[16] were unsuccessful, suggesting that electron detachment (which is not included in the model) is significant, at least at higher energies. The observed cross sections are consistent with facile crossing from the singlet to the triplet surface.

The existence of competing reactions can affect the parameters derived from fits to the data for single products.[16] The ionic products N_2O^- and O^- have sufficiently small cross sections in the threshold region such that they do not affect the fit to the NO^- cross section. While the energy-dependent cross section for electron detachment is not known, the normal fitting parameters for the NO^- product ($n = 1.4$ and maximum cross section $= 1.5$ Å^2) suggest that the shape of the cross section in the threshold region is not significantly affected by electron detachment. The derived threshold is consistent with the apparent threshold after accounting for energy broadening.

Reaction Barrier. The formation of $N_3O_2^-$ is slow in the flow tube. This may be due in part to electron detachment from NO^- [22] or reaction -1 depleting the $NO^-{\cdot}N_2O$ intermediate. There may also be a barrier or a reaction bottleneck for this reaction, which could be attributed to the spin change discussed above. The occurrence of reactions 3 and 5, however, suggest that a barrier to formation of $N_3O_2^-$ is unlikely. Therefore, microscopic reversibility indicates that a barrier in excess of the endothermicity to collision-induced dissociation is also unlikely.

Morris et al.[23] observed reaction 10 in a flow tube and measured rate coefficients of 1.25×10^{-11} cm^3/s at 298 K and 0.90×10^{-11} cm^3/s at 143 K. The only reasonable mechanism for this

$$^{14}NO^- + {}^{14}N^{15}NO \rightarrow {}^{15}NO^- + {}^{14}N^{14}NO \qquad (10)$$

reaction proceeds through the covalent $N_3O_2^-$ structure. The rate coefficients correspond to an approximate efficiency of 1% for this reaction. This reaction also suggests that forming or breaking the covalent bond is moderately slow but barrierless.

Comparison of Dissociative Photodetachment and CID. There are two reasonable explanations for the disagreement between the previous bond energy estimate of 2.0 eV and the much lower value of 0.76 eV derived in this work. The first possibility is that the isomer studied in this work is different from the strongly bound isomer studied by Continetti and coworkers. An isomer bound by 2.0 eV may not be apparent in the present experimental data, since it may have a small cross section for dissociation without electron detachment. However, an isomer bound by 2.0 eV is not consistent with the computational results. It is also unlikely that an isomer with an intermediate bond strength is predominant in the flow tube but not significant in the photodetachment studies.

The second possibility is that essentially none of the dissociative photodetachment products are formed vibrationally cold. This assumption was used to derive the 2.0 eV estimate for the bond energy in $N_3O_2^-$.[12] The difference in energetics implies that nearly every $N_3O_2^-$ ion undergoing dissociative photodetachment gives products with at least ~1.2 eV of internal excitation. In contrast, the CID products are presumed to be formed without vibrational energy at the dissociation threshold.

This can be explained by examining the nature of the excitation processes. Photon absorption gives "vertical" electronic excitation controlled by Franck−Condon factors. Collisional activation in the present energy range results in vibrational excitation. If photodetachment of an electron is a vertical transition, the resulting N_3O_2 neutral will almost certainly have a substantial amount of vibrational energy. This can be approximated in several ways. The vertical detachment energy of N_2O has been calculated to be 1.3 eV.[3] Vertical photodetachment of W-shaped $N_3O_2^-$ should give neutral NO and N_2O in a bent geometry. Classically, this would leave ca. 1.3 eV of vibrational energy in N_2O. Thus, the maximum translational energy release seen by Resat et al.[12] would correspond to a bond energy 1.3 eV lower than the reported value of 2.0 ± 0.2 eV, giving ca. 0.7 eV for an adjusted bond strength. This is consistent with the present results.

A similar approach is to examine the photoelectron spectrum of N_2O^-,[24] which has an N−N−O bond angle actually greater than that computed for $N_3O_2^-$. Photodetachment with 2.54 eV photons gives a peak with an apparent threshold electron kinetic energy of 1.78 eV and a signal maximum at an electron kinetic energy of 1.06 eV.[24] Taking the adiabatic electron affinity of N_2O to be −0.15 eV,[3] this indicates that 1.6 eV of energy is retained in vibrational excitation for a vertical transition, and 0.9 eV is retained at threshold. For photodetachment of $N_3O_2^-$, the 4.66 eV photon energy minus the translational energy is 3.0 eV at the signal maximum and 2.0 eV at the threshold. Subtracting a bond energy of 0.8 eV gives internal energies of 2.2 eV at the signal maximum and 1.2 eV at the threshold. Given the smaller bond angle and greater number of internal degrees of freedom in the $N_3O_2^-$ system, as well as the significantly greater photon energy, these energies are consistent with the values for N_2O.

A third approach to estimating the internal energy sequestration is to use the energy of the neutral N_3O_2 molecule relative to the N_2O + NO products. This has been calculated to be 1.2 eV[13] for the lowest energy geometry, the cis (U-shaped) isomer. Therefore, vertical photodetachment of the presumably W-shaped $N_3O_2^-$ will give a neutral isomer that is more than 1.2 eV higher in energy than the dissociation products. However, some of this energy may be converted into translational energy during dissociation. Thus, the 1.2 eV value could be an overestimate or an underestimate of the internal energy of the dissociation products. Nevertheless, it is consistent with the difference in the experimental results.

The three estimates of the internal energy content of the products of photodissociation of N_2O clearly oversimplify the dynamics of the reaction. However, the agreement of these estimates with the difference in the energetics of the CID and dissociative photodetachment experiments suggests that the basic concept is correct. More detailed dynamics simulations would help explain the surprisingly large amount of energy remaining in product vibrational degrees of freedom in the photodissociation experiments.

Acknowledgment. We thank Rainer Dressler, Robert Continetti, and James Coe for very helpful discussions of this work. Peter Armentrout, Kent Ervin, and Mary Rodgers are thanked for developing the improved version of the CRUNCH data analysis program. We also thank the DeKalb, IL, Police Department for the donation of five confiscated cylinders of N_2O to the NIU chemistry department. The Undergraduate Research Apprenticeship Program at NIU provided partial funding for this work. Acknowledgment is made to the donors of the Petroleum Research Fund, administered by the American Chemical Society, for partial support of this research.

References and Notes

(1) Travers, M. J.; Cowles, D. C.; Ellison, G. B. *Chem. Phys. Lett.* **1989**, *164*, 449.

(2) McCarthy, M. C.; Allington, J. W. R.; Griffith, K. S. *Chem. Phys. Lett.* **1998**, *289*, 156−159.

(3) McCarthy, M. C.; Allington, J. W. R.; Sullivan, K. O. *Mol. Phys.* **1999**, *96*, 1735−1737.

(4) The related anion $N_3O_4^-$ (dinitramide) has also been studied: Schmitt, R. J.; Krempp, M.; Bierbaum, V. M. *Int. J. Mass Spectrom. Ion Processes* **1992**, *117*, 621−632. Dinitraminic acid is one of the strongest gas-phase acids.

(5) Moruzzi, J. L.; Dakin, J. T. *J. Chem. Phys.* **1968**, *49*, 5000−5006.

(6) Parkes, D. A. *J. Chem. Soc., Faraday Trans. 1* **1972**, *68*, 2103−2120. Parkes, D. A. *J. Chem. Soc., Faraday Trans. 1* **1972**, *68*, 2121−2128.

(7) Viggiano, A. A.; Morris, R. A.; Paulson, J. F. *J. Phys. Chem.* **1990**, *94*, 3286−3290.

(8) Marx, R.; Mauclaire, G.; Fehsenfeld, F. C.; Dunkin, D. B.; Ferguson, E. E. *J. Chem. Phys.* **1973**, *58*, 3267−3273.

(9) Hiraoka, K.; Fujimaki, S.; Kazuo, A.; Yamabe, S. *J. Phys. Chem.* **1994**, *98*, 8295−8301.

(10) Coe, J. V.; Snodgrass, J. T.; Freidhoff, C. B.; McHugh, K. M.; Bowen, K. H. *J. Chem. Phys.* **1987**, *87*, 4302−4309.

(11) Hayakawa, S.; Matsumoto, A.; Yoshioka, M.; Matsuoka, S.; Sugiura, T. *Mass Spectrosc. (Tokyo)* **1986**, *34*, 147−158.

(12) Resat, M. S.; Zengin, V.; Garner, M. C.; Continetti, R. E. *J. Phys. Chem. A* **1998**, *102*, 1719−1724.

(13) Pápai, I.; Stirling, A. *Chem. Phys. Lett.* **1996**, *253*, 196−200.

(14) Gerlich, D. *Adv. Chem. Phys.* **1992**, *82*, 1−176.

(15) Do, K.; Klein, T. P.; Pommerening, C. A.; Sunderlin, L. S. *J. Am. Soc. Mass Spectrom.* **1997**, *8*, 688−696.

(16) Ervin, K. M.; Loh, S. K.; Aristov, N.; Armentrout, P. B. *J. Phys. Chem.* **1983**, *87*, 3593−3596. Ervin, K. M.; Armentrout, P. B. *J. Chem. Phys.* **1985**, *83*, 166−189. Rodgers, M. T.; Ervin, K. M.; Armentrout, P. B. *J. Chem. Phys.* **1997**, *106*, 4499−4508. Rodgers, M. T.; Armentrout, P. B. *J. Chem. Phys.* **1998**, *109*, 1787−1800.

(17) The theoretical justification for this cross section form is discussed in: Rebick, C.; Levine, R. D. *J. Chem. Phys.* **1973**, *58*, 3942−3952. Aristov. N.; Armentrout, P. B. *J. Am. Chem. Soc.* **1986**, *108*, 1806−1819.

(18) Loh, S. K.; Hales, D. A.; Lian, L.; Armentrout, P. B. *J. Chem. Phys.* **1989**, *90*, 5466. Schultz, R. H.; Crellin, K. C.; Armentrout, P. B. *J. Am. Chem. Soc.* **1991**, *113*, 8590.

(19) Frisch, M. J.; Trucks, G. W.; Schlegel, H. B.; Gill, P. M. W.; Johnson, B. G.; Robb, M. A.; Cheeseman, J. R.; Keith, T. A.; Peterson, G. A.; Montgomery, J. A.; Raghavachari, K.; Al-Laham, V. G.; Zakrzewski, V. G.; Oritz, J. V.; Foresman, J. B.; Ciolowski, J.; Stefanov, B. B.;

Nanayakkara, A.; Challacombe, M.; Peng, C. Y.; Ayala, P. Y.; Chen, W.; Wong, M. W.; Andres, J. L.; Replogle, E. S.; Gomperts, R.; Martin, R. L.; Fox, D. J.; Binkley, J. S.; DeFrees, D. J.; Baker, J.; Stewart, J. P.; Head-Gordon, M.; Gonzalez, C.; Pople, J. A. GAUSSIAN 94, Rev. B; Gaussian, Inc.: Pittsburgh, PA 1995.

(20) Dunning, T. H., Jr. *J. Chem. Phys.* **1989**, *90*, 1007−1023. Kendall, R. A.; Dunning, T. H., Jr.; Harrison, R. J. *J. Chem. Phys.* **1992**, *96*, 6796−6806.

(21) Bastian, M. J.; Dressler, R. A.; Levandier, D. J.; Murad, E.; Muntean, F.; Armentrout, P. B. *J. Chem. Phys.* **1997**, *106*, 9570−9579.

(22) McFarland, M.; Dunkin, D. B.; Fehsenfeld, F. C.; Schmeltekopf, A. L.; Ferguson, E. E. *J. Chem. Phys.* **1972**, *56*, 2358−2365.

(23) Morris, R. A.; Viggiano, A. A.; Paulson, J. F. *J. Chem. Phys.* **1990**, *92*, 2342−2343.

(24) Coe, J. V.; Snodgrass, J. T.; Freidhoff, C. B.; McHugh, K. M.; Bowen, K. H. *Chem. Phys. Lett.* **1986**, *124*, 274−277.